

# HYDRODYNAMICS OF ELECTROCHEMICAL CELLS WITH A ROTATING SEMI-SPHERICAL ELECTRODE

**Rachel Manhães de Lucena, rachel.lucena@gmail.com**

Metallurgy and Materials Engineering Department – Federal University of Rio de Janeiro, PO Box 68505, 21941-972 Rio de Janeiro, RJ, Brazil

**Gustavo R. Anjos, gustavo.rabello@gmail.com**

Group of Environmental Studies for Water Reservatories – GESAR/State University of Rio de Janeiro, Rua Fonseca Teles 121, 20940-200, Rio de Janeiro, RJ, Brazil

**Norberto Mangiavacchi, norberto.mangiavacchi@gmail.com**

Group of Environmental Studies for Water Reservatories – GESAR/State University of Rio de Janeiro, Rua Fonseca Teles 121, 20940-200, Rio de Janeiro, RJ, Brazil

**José Pontes, jopontes@metalmat.ufrj.br**

Metallurgy and Materials Engineering Department – Federal University of Rio de Janeiro, PO Box 68505, 21941-972 Rio de Janeiro, RJ, Brazil

**Abstract.** We propose a numerical model to obtain results for the velocity and concentration profiles close to semi-spherical rotating electrodes in electrochemical cells. The profiles refer to nondimensional velocity components along the radial direction, for straight lines ranging from angles with the rotating axis  $0 < \theta < \pi/2$  obtained by solving the Navier-Stokes equations using the finite element method. The discretization of the domain is made with an object oriented approach. Spatial discretization of diffusive terms and the pressure is made by the Galerkin method. For the material derivative we use a semi-lagrangian method.

**Keywords:** Corrosion, Rotating Disk Flow, Semi-spherical Electrode, Finite Element Method

## 1. INTRODUCTION

In the last 15 years, the group of Applied Electrochemistry of the Federal University of Rio de Janeiro (PEMM/COPPE/UFRJ) has been involved with studies on the hydrodynamics of electrochemical cells having rotating disk electrodes and, in a lesser extent, semi-spherical rotating electrodes, we mention [Godinez \(1996\)](#), [Barcia et al. \(1998\)](#), [Anjos \(2007\)](#) and [Oliveira \(2011\)](#). Rotating disk flow is described by a similarity solution found by [von Kármán \(1921\)](#) through which the original governing PDEs are transformed in a system of nonlinear ODEs. Due to the existence of this similarity solution rotating

disk flow has been widely used as a prototype not only in electrochemistry, but also in other domains, like high speed aerodynamics. The use of rotating disk electrodes present a limitation resulting from the fact that the electrode surface loses its original geometry due to the dissolution of the iron in the acid media of the electrolyte. An alternative configuration consists in employing semi-spherical electrodes, which keep their geometry when dissolved. However, a major challenge appears in the theoretical approach of the problem, due to the fact that a similarity solution of the hydrodynamics no longer exists for the hydrodynamic field close to a rotating sphere.

In 1996, a doctoral thesis developed in the group of applied electrochemistry of the Federal University of Rio de Janeiro dealt with a theoretical study for the hydrodynamic

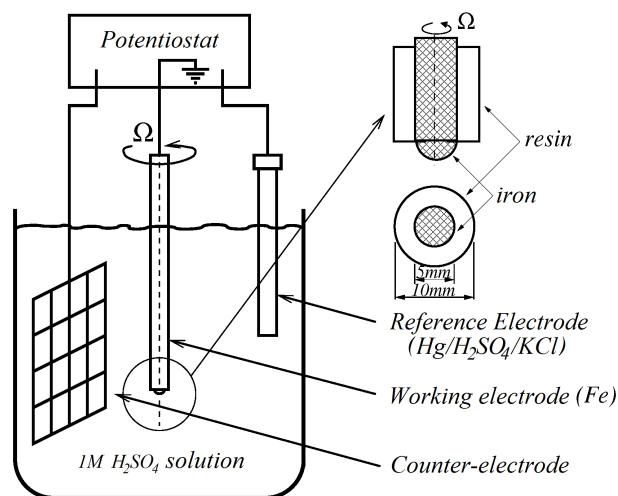


Figure 1. Electrochemical cell with a rotating semi-spherical electrode

and the concentration fields of a chemical species, close to a semi-spherical electrode. Two approaches were employed to describe both fields. In the first one the governing PDEs including the simplifications introduced by the particular geometry were solved numerically and in the second one a series expansion of the velocity components in functions depending on the radial coordinate  $r$  was developed.

The subject electrochemical cell comprises a semi-spherical working electrode immersed in a 1M of  $\text{S}_2\text{OH}_4$  electrolyte solution, turning with specified  $\bar{\Omega}$  angular velocity, a counter-electrode and a reference electrode, as schematically sketched in Fig.1.

The governing equations for an incompressible fluid, written in nondimensional form read:

$$\frac{D\mathbf{v}}{Dt} = -\frac{1}{\rho}\nabla p + \frac{1}{Re}\nabla \cdot [(\nabla\mathbf{v} + \nabla\mathbf{v}^T)] \quad (1)$$

$$\nabla \cdot \mathbf{v} = 0 \quad (2)$$

$$\frac{Dc}{Dt} = \frac{1}{ReSc}\nabla \cdot (D\nabla c). \quad (3)$$

In the above equations,  $c$  is the concentration of the chemical species resulting from the dissolution of the iron electrode in the electrolyte,  $D$  is the diffusion coefficient of the species,  $Re$  and  $Sc$  are the Reynolds and Schmidt numbers, respectively.

The hydrodynamic equations with the simplifications introduced by the geometry of the rotating semi-sphere read:

$$\frac{\partial v_r}{\partial r} + \frac{1}{r_0}\frac{\partial v_\theta}{\partial \theta} + \frac{\cot \theta}{r_0}v_\theta = 0 \quad (4)$$

$$v_r\frac{\partial v_\theta}{\partial r} + \frac{v_\theta}{r_0}\frac{\partial v_\theta}{\partial \theta} - \frac{\cot \theta}{r_0}v_\phi^2 = \nu\frac{\partial^2 v_\theta}{\partial r^2} \quad (5)$$

$$v_r\frac{\partial v_\phi}{\partial r} + \frac{v_\theta}{r_0}\frac{\partial v_\phi}{\partial \theta} + \frac{\cot \theta}{r_0}v_\theta v_\phi = \nu\frac{\partial^2 v_\phi}{\partial r^2}. \quad (6)$$

In the above equations,  $r_0$  is the radius of the semi-sphere and  $\nu$ , the kinematic viscosity of the fluid. Boundary conditions for Eqs. (4)-(6) are, in  $r = r_0$ :  $v_r = v_\theta = 0$  and  $v_\phi = r_0\bar{\Omega}\sin \theta$ , where  $\bar{\Omega}$  is the steady angular velocity imposed to the electrode.

A solution of Eqs. (4)-(6) in a power series of  $\theta$  is given by:

$$v_\theta = r_0\bar{\Omega}F(\theta, \eta) = r_0\bar{\Omega} [\theta F_1(\eta) + \theta^3 F_3(\eta) + \theta^5 F_5(\eta) + \theta^7 F_7(\eta) + \dots] \quad (7)$$

$$v_\phi = r_0\bar{\Omega}G(\theta, \eta) = r_0\bar{\Omega} [\theta G_1(\eta) + \theta^3 G_3(\eta) + \theta^5 G_5(\eta) + \theta^7 G_7(\eta) + \dots] \quad (8)$$

$$v_r = (\nu\bar{\Omega})^{1/2} H(\theta, \eta) = (\nu\bar{\Omega})^{1/2} [H_1(\eta) + \theta^2 H_3(\eta) + \theta^4 H_5(\eta) + \theta^6 H_7(\eta) + \dots], \quad (9)$$

where  $\eta$  is defined by:  $\eta = (\bar{\Omega}/\nu)^{1/2}(r - r_0)$  and  $F_n$ ,  $G_n$  and  $H_n$ , for  $n = 1, 3, 5, 7, \dots$ , are nondimensional functions.

Godinez' expansion provides numerically stable solutions of Eqs. (7)-(9) not too close to the sphere equator, namely, for angles  $\theta < 80^\circ$ , but the results for  $\theta > 80^\circ$  are not satisfactory. The purpose of this work is to extend Godinez' results and obtain numerical solutions of the full 3-dimensional equations governing the hydrodynamic and the concentration field of the chemical species originated by dissolution of the semi-spherical iron electrode.

## 2. FINITE ELEMENT METHOD

The Finite Element Method (FEM) provides a tool for discretizing and solving the original PDEs. The domain is subdivided in small subdomains denoted by finite elements. The ensemble of finite elements define the numerical grid. In short, the method consists in finding an approximate solution of the weak or variational form of the governing equations through the finite element interpolation functions.

## 2.1 Variational Formulation

The variational formulation is obtained by properly weighting the governing equations, namely, Eqs.(1)-(3). We obtain:

$$\int_{\Omega} \frac{D\mathbf{v}}{Dt} \cdot \mathbf{w} d\Omega - \frac{1}{\rho} \int_{\Omega} p [\nabla \cdot \mathbf{w}] d\Omega + \frac{1}{Re} \int_{\Omega} [(\nabla \mathbf{v} + \nabla \mathbf{v}^T)] : \nabla \mathbf{w}^T d\Omega = 0 \quad (10)$$

$$\int_{\Omega} [\nabla \cdot \mathbf{v}] q d\Omega = 0 \quad (11)$$

$$\int_{\Omega} \frac{Dc}{Dt} r d\Omega + \frac{1}{ReSc} \int_{\Omega} (D\nabla c) \cdot \nabla r^T d\Omega = 0. \quad (12)$$

Functions  $\mathbf{w}$ ,  $q$  and  $r$  are the *weighting functions* defined in the space  $\mathcal{V}$  with the prescription:  $\mathcal{V} := \{\mathbf{w} \in \mathcal{H}^1(\Omega) \mid \mathbf{w} = 0 \text{ in } \Gamma_c\}$ , where  $\mathbf{u}_c$  is the *essential boundary condition* value,  $\Gamma_c$  a possible boundary for the domain  $\Omega$ ,  $\mathcal{H}^1(\Omega) := \left\{ \mathbf{u} \in \mathcal{L}^2(\Omega) \mid \frac{\partial \mathbf{u}}{\partial x_i} \in \mathcal{L}^2(\Omega), i = 1, \dots, n \right\}$  and  $\mathcal{L}^2(\Omega)$  is the *Lebesgue space*, i. e., the space of all *square integrable* functions. Boundary conditions for this work are:  $v_r = v_{\theta} = 0$  and  $v_{\phi} = r_0 \bar{\Omega} \sin \theta$ , where  $\bar{\Omega}$  is the steady angular velocity imposed to the electrode. These conditions approximately mimic an unbounded domain in the radial direction.

## 2.2 The Semi-discrete Galerkin Method

The semi-discrete Galerkin Method provides a partial discretization where the functions that approximate a solution for the governing equations (Eqs.(10)-(12)) comprise a linear combination of shape functions depending on the time of functions intended to depend on the space coordinates. Following this procedure we denote by  $NV$ ,  $NP$  and  $NC$  the number of velocity, pressure and concentration nodes, respectively, of the discrete grid of elements of the original domain  $\Omega$ . The following semi-discrete approximation functions are obtained:

$$\begin{aligned} v_x(\mathbf{x}, t) &\approx \sum_{i=1}^{NV} u_i(t) N_i(\mathbf{x}), & v_y(\mathbf{x}, t) &\approx \sum_{i=1}^{NV} v_i(t) N_i(\mathbf{x}), & v_z(\mathbf{x}, t) &\approx \sum_{i=1}^{NV} w_i(t) N_i(\mathbf{x}), \\ p(\mathbf{x}, t) &\approx \sum_{i=1}^{NP} p_i(t) P_i(\mathbf{x}) & \text{and} & & c(\mathbf{x}, t) &\approx \sum_{i=1}^{NC} c_i(t) C_i(\mathbf{x}), \end{aligned}$$

where the coefficients  $u_i, v_i, w_i, p_i$  e  $c_i$  denote continuous functions in the time ( $t$ ) and functions  $N_i(\mathbf{x})$ ,  $P_i(\mathbf{x})$  and  $C_i(\mathbf{x})$  are interpolation functions at specified positions  $\mathbf{x}$  for the velocity, pressure and concentration, respectively.

The discretized system becomes, in matrix form:

$$\begin{aligned} \mathbf{M}\dot{\mathbf{v}} + \frac{1}{Re} \mathbf{K}\mathbf{v} - \mathbf{G}\mathbf{p} &= 0 \\ \mathbf{D}\mathbf{v} &= 0 \\ \mathbf{M}_c\dot{\mathbf{c}} + \frac{1}{ReSc} \mathbf{K}_c\mathbf{c} &= 0, \end{aligned}$$

where

$$\begin{aligned} \mathbf{M} &= \begin{bmatrix} \mathbf{M}_x & 0 & 0 \\ 0 & \mathbf{M}_y & 0 \\ 0 & 0 & \mathbf{M}_z \end{bmatrix}, & \mathbf{K} &= \begin{bmatrix} \mathbf{K}_x & \mathbf{K}_{xy} & \mathbf{K}_{xz} \\ \mathbf{K}_{yx} & \mathbf{K}_y & \mathbf{K}_{yz} \\ \mathbf{K}_{zx} & \mathbf{K}_{zy} & \mathbf{K}_z \end{bmatrix}, & \mathbf{G} &= \begin{bmatrix} \mathbf{G}_x & \mathbf{G}_y & \mathbf{G}_z \end{bmatrix}^T, \\ \mathbf{K}_x &= 2\mathbf{K}_{xx} + \mathbf{K}_{yy} + \mathbf{K}_{zz}, & \mathbf{K}_y &= \mathbf{K}_{xx} + 2\mathbf{K}_{yy} + \mathbf{K}_{zz}, & \mathbf{K}_z &= \mathbf{K}_{xx} + \mathbf{K}_{yy} + 2\mathbf{K}_{zz}, \\ \mathbf{D} &= \begin{bmatrix} \mathbf{D}_x & \mathbf{D}_y & \mathbf{D}_z \end{bmatrix}, & \dot{\mathbf{v}} &= \begin{bmatrix} \dot{\mathbf{u}} & \dot{\mathbf{v}} & \dot{\mathbf{w}} \end{bmatrix}^T, & \mathbf{v} &= \begin{bmatrix} \mathbf{u} & \mathbf{v} & \mathbf{w} \end{bmatrix}^T, \\ \mathbf{M}_c &= \begin{bmatrix} \mathbf{M}_c & 0 & 0 \\ 0 & \mathbf{M}_c & 0 \\ 0 & 0 & \mathbf{M}_c \end{bmatrix} & \text{and} & \mathbf{K}_c &= \begin{bmatrix} \mathbf{K}_{cxx} & 0 & 0 \\ 0 & \mathbf{K}_{cyy} & 0 \\ 0 & 0 & \mathbf{K}_{czz} \end{bmatrix}. \end{aligned}$$

### 2.3 The semi-lagrangean method

The method considered in this section has been widely used since the 80's in the solution of convective problems. The main favorable features are stability and the large time steps allowed.

One can observe the use of a discrete representation of the substantial derivative in the discretized weak form of the governing equations. In this section we apply the semi-lagrangean method to the substantial derivatives of the governing equations. We obtain:

$$\frac{D\mathbf{v}}{Dt} = \frac{\mathbf{v}_i^{n+1} - \mathbf{v}_d^n}{\Delta t} \quad (13)$$

The global matrix system takes the following discrete form:

$$\mathbf{M} \left( \frac{\mathbf{v}_i^{n+1} - \mathbf{v}_d^n}{\Delta t} \right) + \frac{1}{Re} \mathbf{K} \mathbf{v}^{n+1} - \mathbf{G} p^{n+1} = 0 \quad (14)$$

$$\mathbf{D} \mathbf{v}^{n+1} = 0 \quad (15)$$

$$\mathbf{M}_c \left( \frac{c_i^{n+1} - c_d^n}{\Delta t} \right) + \frac{1}{ReSc} \mathbf{K}_c c^{n+1} = 0, \quad (16)$$

where  $\mathbf{v}_d^n = \mathbf{v}^n(x_d, t^n)$ ,  $c_d^n = c^n(x_d, t^n)$  and  $x_d$  refers to the starting point in the time  $t^n \leq t \leq t^{n+1}$  with initial condition  $x(t^{n+1}) = x_i$ .

### 3. RESULTS

Figure 2(a) shows the numerical grid used in the FEM simulations of the hydrodynamic field close to the semi-spherical electrode. Boundary conditions assume vanishing velocity at the bottom and at the upper free surface. At the electrode surface the fluid turns with the tangential velocity of the semi-sphere. At the sidewalls we specify  $p = 0$ , a condition that better mimics an infinite domain in the horizontal plane. Fig. 2(b) shows a section along the  $x$  direction in  $\mathbb{R}^3$ .

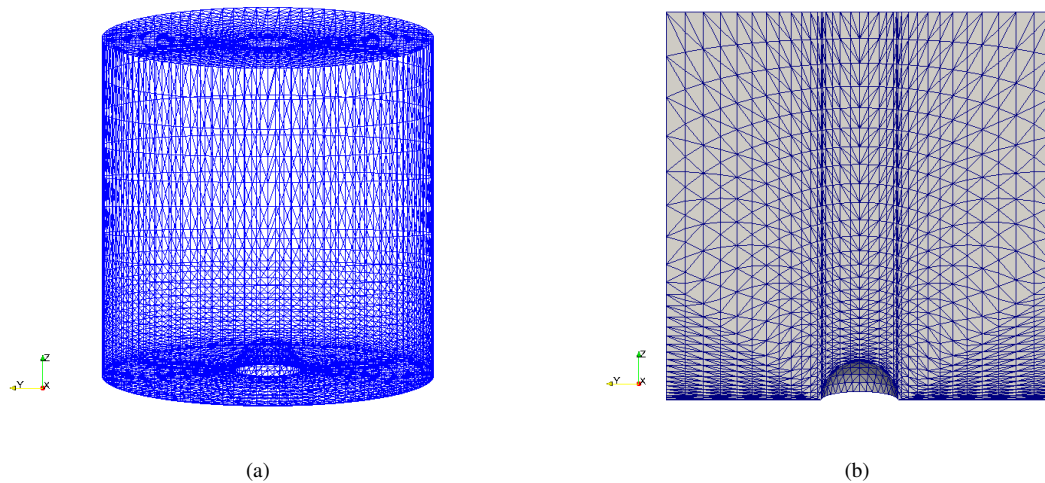


Figure 2. (a) Representation of computational mesh; (b) Sectioned mesh

Figure 3 shows the distribution velocity magnitude at two different times. Figure 3(a) at time  $t = 0.3$  shows the radial development of a boundary layer in the neighbourhood of the equator. Figure 3(b) shows the further development of boundary layer towards the lateral boundaries of the domain.

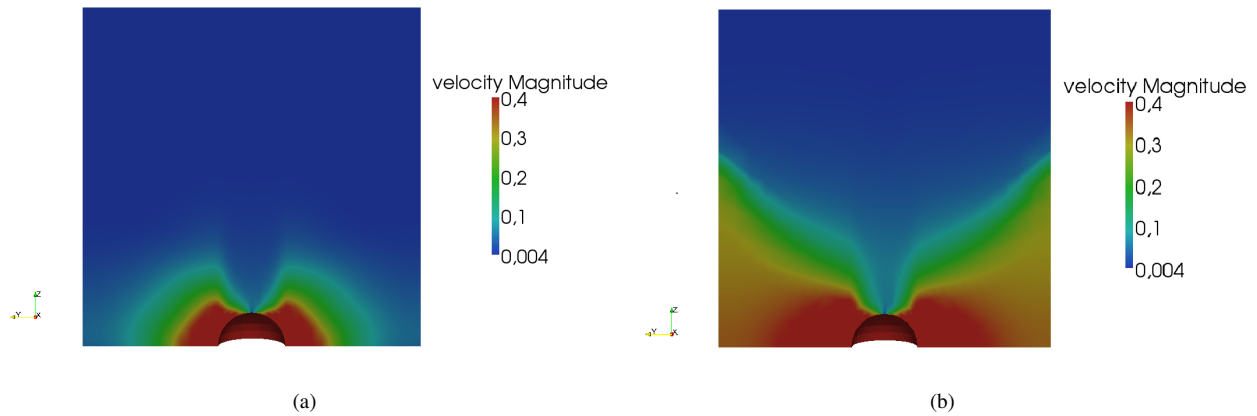


Figure 3. (a) Velocity magnitude at time  $t = 0.3$ ; (b) Velocity magnitude at time  $t = 5.0$

Figure 4 shows the distribution  $z$  component of the velocity at two different times. Figure 4(a) at time  $t = 0.3$  shows the development of a negative velocity close to the pole due to the rotation of the semi-sphere. Figure 4(b) shows the grows of this region towards the lateral boundaries of the domain, and the formation of stagnation regions close to the equator.

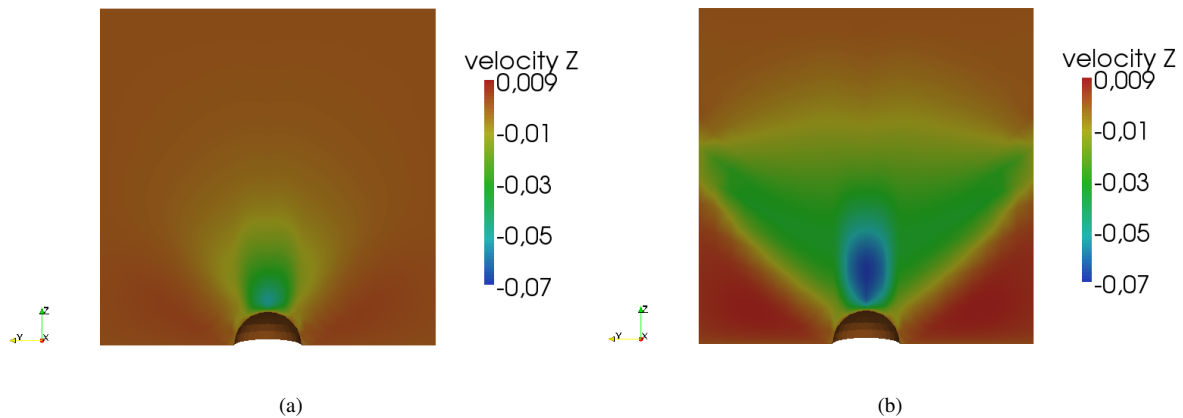


Figure 4. (a)  $z$  component of the velocity at time  $t = 0.3$ ; (b)  $z$  component of the velocity at time  $t = 5.0$

Figure 5 shows the distribution  $y$  component of the velocity at the  $yz$  plane at two different times. Figure 5(a) at time  $t = 0.3$  shows the development of a thin boundary layer from the pole to the equator and then a jet detaching from the equator. Figure 5(b) shows the development of the boundary layer and the jet at later time.

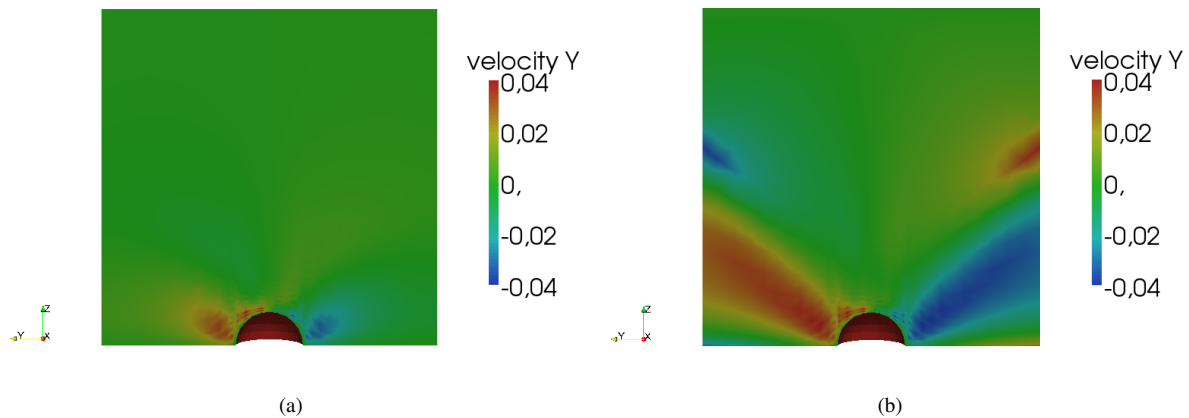


Figure 5. (a)  $y$  component of the velocity at the  $yz$  plane at time  $t = 0.3$ ; (b)  $y$  component of the velocity at the  $yz$  plane at time  $t = 5.0$

Fig.6 shows the stream lines obtained by solving the governing equations employing the method described in Sec.2. . The stream lines start from the bulk of the flow swirling in the direction of the semi-sphere and then the detach from boundary layer and are ejected outwards.

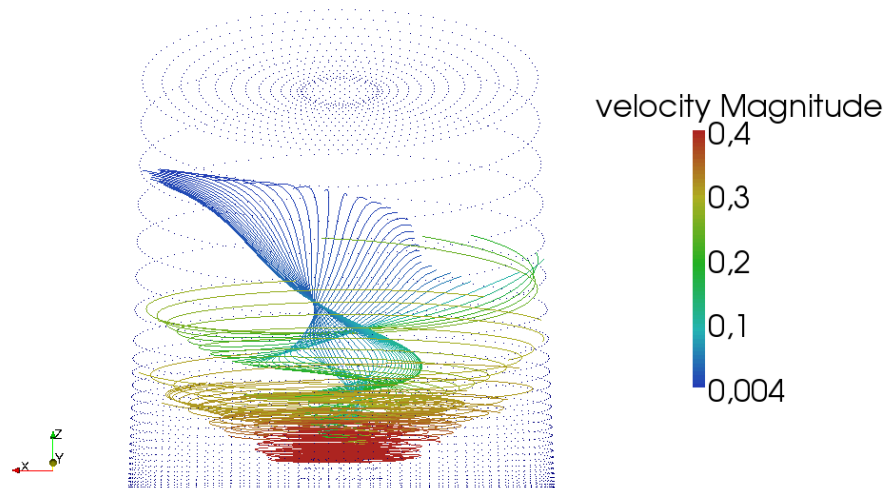


Figure 6. Stream lines

The results are physically consistent with previous results obtained for electrochemical cells with rotating semi-spherical electrodes. We will proceed investigating the influence of mesh refining and domain dimensions on the flow.

#### 4. ACKNOWLEDGMENTS

The authors acknowledge financial support from the Brazilian agencies FAPERJ and CNPq. They also acknowledge the Group of Environmental Studies for Water Reservoirs – GESAR/State University of Rio de Janeiro, where most simulations here presented were performed.

## 5. REFERENCES

- Anjos, G.R., 2007. *Solução do campo hidrodinâmico em células eletroquímicas pelo método dos elementos finitos*. M.Sc. dissertation, COPPE/UFRJ, Rio de Janeiro, RJ, Brazil.
- Barcia, O.E., Godinez, J.S., Lamego, L., Mattos, O.R. and Tribollet, B., 1998. “Rotating hemispherical electrode - accurate expressions for the limiting current and the convective warbug impedance”. *Journal Electrochemical Society*, Vol. 145, No. 12, pp. 4189–4195.
- Barcia, O., Mangiavacchi, N., Mattos, O. and Tribollet, B., 2000. “Rotating disk flow in electrochemical cells: A coupled solution for hydrodynamic and mass equations”. *Journal of The Electrochemical Society*, Vol. 155, No. 5, pp. 424–427.
- Godinez, J.G.S., 1996. *Eletrodo semi-esférico rotatório: teoria para o estado estacionário*. D.Sc. thesis, COPPE/UFRJ, Rio de Janeiro, RJ, Brazil.
- Mangiavacchi, N., P.J.B.O.E., 2007. “Rotating-disk flow stability in electrochemical cells: Effect of the transport of a chemical species”. *Physics of Fluids*, Vol. 19, pp. 114–119.
- Oliveira, G.C.P., 2011. *Estabilidade hidrodinâmica em células eletroquímicas pelo método de elementos finitos*. M.Sc. dissertation, COPPE/UFRJ, Rio de Janeiro, RJ, Brazil.
- von Kármán, T, Z.A., 1921. “Über laminare and turbulente reibung”. *ZAMM*, Vol. 1, pp. 233–252.

## 6. RESPONSIBILITY NOTICE

The following text, properly adapted to the number of authors, must be included in the last section of the paper: The author(s) is (are) the only responsible for the printed material included in this paper.